Remote Sens. **2011**, *3*, 2346-2363; doi:10.3390/rs3112346

OPEN ACCESS

Remote Sensing

ISSN 2072-4292

www.mdpi.com/journal/remotesensing

Article

Estimating Crown Variables of Individual Trees Using Airborne and Terrestrial Laser Scanners

Sung-Eun Jung [1], Doo-Ahn Kwak [2], Taejin Park [2], Woo-Kyun Lee [2,*] and Seongjin Yoo [2]

[1] Department of Environment & Marine Information, Sundosoft, Seoul 153-759, Korea; E-Mail: truthse@gmail.com

[2] Division of Environmental Science and Ecological Engineering, Korea University, Seoul 136-701, Korea; E-Mails: tulip96@korea.ac.kr (D.-A.K.); taejin1392@korea.ac.kr(T.P.); yoosjin@gmail.com (S.Y.)

* Author to whom correspondence should be addressed; E-Mail; leewk@korea.ac.kr; Tel.: +82-2-3290-3016; Fax: +82-2-3290-3470.

Received: 26 August 2011; in revised form: 7 September 2011 / Accepted: 21 October 2011 / Published: 28 October 2011

Abstract: In this study, individual tree height (TH), crown base height (CBH), crown area (CA) and crown volume (CV), which were considered as essential parameters for individual stem volume and biomass estimation, were estimated by both an airborne laser scanner (ALS) and a terrestrial laser scanner (TLS). These ALS- and TLS-derived tree parameters were compared because TLS has been introduced as an instrument to measure objects more precisely. ALS-estimated TH was extracted from the highest value within a crown boundary delineated with the crown height model (CHM). The ALS-derived CBH of individual trees was estimated by *k*-means clustering method using the ALS data within the boundary. The ALS-derived CA was calculated simply with the crown boundary, after which CV was computed automatically using the crown geometric volume (CGV). On the other hand, all TLS-derived parameters were detected manually and precisely except the TLS-derived CGV. As a result, the ALS-extracted TH, CA, and CGV values were underestimated whereas CBH was overestimated when compared with the TLS-derived parameters. The coefficients of determination (R^2) from the regression analysis between the ALS and TLS estimations were approximately 0.94, 0.75, 0.69 and 0.58, and root mean square errors (RMSEs) were approximately 0.0184 m, 0.4929 m, 2.3216 m^2 and 13.2087 m^3 for TH, CBH, CA and CGV, respectively. Thereby, the error rate decreased to 0.0089, 0.0727 and 0.0875 for TH, CA and CGV via the combination of ALS and TLS data.

Keywords: airborne laser scanner; terrestrial laser scanner; digital canopy model; k-means clustering; crown geometric volume

1. Introduction

Forest inventory information has always been important with respect to forest management. For sustainable forest management, more information is needed, not only for planning future forest management, but also for recording the previous status of the forested area [1]. However, the traditional methods of investigating forest parameters such as tree height (TH), crown base height (CBH), diameter at breast height (DBH), and crown diameter (CD), involve labor-intensive forest inventories, the incorporation of complex sampling designs, and supplementary work [2,3].

Recently, optical remote sensing techniques using aerial photographs and satellite imagery have either supplemented or supplanted some of such field measurements. The application of optical remote sensing techniques enables the measurement of forest growth factors, and ecological and environmental information over wide areas [4]. However, remote sensing using optical sensors, except stereo-image analysis of the forest, suffers from the limitation of restricted time and cost when stand information for three-dimensional vertical structures is extracted [5].

On the other hand, airborne laser scanners (ALS) can be used to acquire vertical and horizontal forest structure in detail as scanning targets with laser pulses [6]. In particular, such vertical measurements enable the prediction of forest biomass and carbon storage. Furthermore, laser sensors can be used to accurately measure topographical information, the physical properties of a forest and other information. Therefore, ALS has been recognized as a more efficient and precise instrument than field surveys and optical remote sensing techniques [4,7]. Since the early to mid 1980s, several studies using full waveform sensors have been performed for forest inventory [8], merchantable timber volume estimation [9], and forest canopy characterization [10]. Recently, several researchers have applied discretely emitted laser pulses for the individual- and stand-level TH estimation [5,11-13] and height-based timber volume estimates [14,15].

However, the estimation of forest structural parameters using discrete pulses suffers from a few problems such as tree density, crown overlapping, and missing tree tops and small canopy elements [16]. High tree density causes crown edge overlapping between neighboring trees, leading to the underestimation of crown diameter, area and volume in such forest areas. Moreover, it is actually hard for laser pulses to be reflected on correct tree tops because the density of the returns is insufficient for the detection of individual trees [17]. Therefore, ALS estimates of TH tend to slightly be underestimated when compared with field measurements. ALS data, with minimum footprint sizes of 0.1 m and 0.25 m, may not be useful for detecting small canopy elements [18,19]. In addition, the crown edge overlapping can cause another error when estimating DBH, CBH, and CD [16]. For supplementing such underestimation, many researchers have used regression models using the correlation between field- and ALS-derived biophysical variables.

On the other hand, a few researchers have used terrestrial laser scanner (TLS) which enables the precise assessments of forest structure. However, as the procedure for data acquisition by TLS is

intensive due to inaccessible and broad forest area, it has only been conducted over relatively small sample plots [20-22] by considering the condition of the target area.

To overcome the drawbacks of both instruments, we tried to combine ALS and TLS data in sample plots in order to estimate forest growth factors such as TH, CBH, CA and crown geometric volume (CGV). These parameters were effectively adopted for individual stem volume and biomass estimation, because it can reduce the difficulties from regression analysis between DBH and CA [5,23]. Thereby, the ALS-derived results were supplemented with precise TLS-derived data that could be extended to a broad area. In particular, all supplements used in the ALS estimation were calculated based on the assumption that the TLS-derived estimation was more precise than that by field measurement [20,24,25]. The study results revealed that more accurate estimates of the examined forest parameters were obtained via the combined ALS and TLS data procedure than when only ALS data were used independently.

2. Materials

2.1. Study Area

The study area was located at Gwangneung Experimental Forest of the Korea Forest Research Institute (KFRI) in central South Korea (Datum: Geodetic Reference System 1980 (GRS80), Coordinates: upper left 127°09′25.864″E, 37°45′46.265″N and lower right 127°10′44.629″E, 37°44′10.201″E) (Figure 1). The study area elevation ranged from 160 to 573 m above sea level and was dominated by steep hills, with the main tree species of Red Pine (*Pinus densiflora*), Korean Pine (*Pinus koraiensis*), Japanese Larch (*Larix leptolepis*) and Oaks (*Quercus* spp.). Korean Pine stands were cautiously selected, and 30 trees were investigated for regression model (15 trees) and its verification (15 trees). Undetectable small trees were not employed to avoid the characteristic drawback that the crowns of trees under other trees cannot be recognized properly by ALS. Selected stands were composed of homogeneous Korean Pines with low density.

Figure 1. Digital aerial photograph of the study area acquired on 3 April 2007.

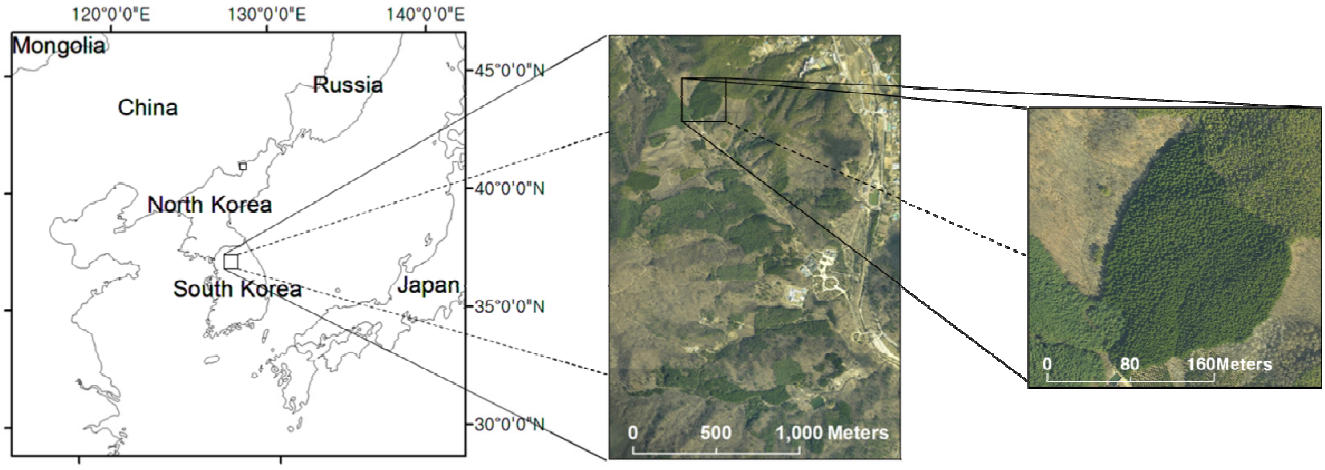

2.2. Acquisition of Airborne Laser Scanner Data

ALTM 3070 (a small footprint LiDAR system) by Optech Inc. was used to acquire the ALS data, and the flight was performed on 3 April 2007. The ALS data were acquired from an altitude of 1,400 m, with a sampling density of 5~10 points per square meter. The radiometric resolution, scan frequency and scan width were 12 bits, 70 Hz and ±25°, respectively. The acquired ALS data were classified into ground- and above-ground returns using Terra Scan software's automatic procedure.

2.3. Acquisition of Terrestrial Laser Scanner Data

TLS scanning work was performed on 10 October 2008 using GS200 3D Scanner by Trimble Inc. (Table 1). The TLS data were acquired from approximately 30 m away to obtain all vertical components of one tree from bottom to top because the vertical movement of GS200 3D Scanner had an angle limitation of up to 38° and down to 22° [26].

Table 1. Descriptive statistics of the terrestrial laser scanner (TLS) measurements.

Measured Parameters	N/ha	Max.	Min.	Mean	SD
Tree height (m)	427	26.8	18.0	22.3	2.3
DBH (cm)		49.7	21.7	32.1	6.3
Crown base height (m)		20.2	12.7	16.2	1.9
Crown width (m)		6.7	4.4	5.5	0.7

Figure 2. Acquisition of TLS data from four directions for measuring the whole shape of the single target tree.

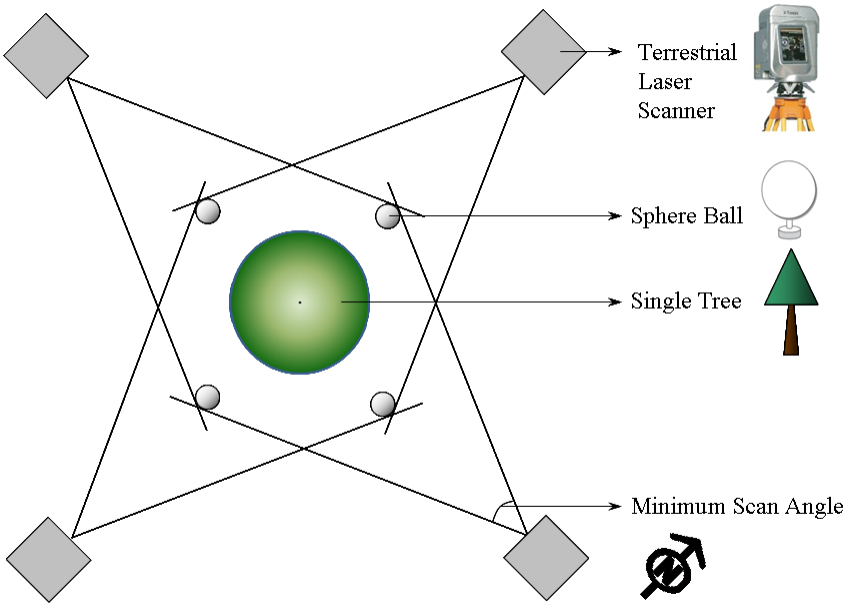

Each tree was measured in the four compass directions in order to materialize the three dimensional shape of the tree because single direction laser scanning work is incapable of acquiring information of an opposite side (Figure 2). Moreover, the measurements were conducted in a relatively flat area to

avoid uncertainty errors. When the data were obtained, the scanning speed, interval between reflected returns and tolerance of the laser scanner were set at 5,000 pts/s, 3 mm at 100 m and 3 mm at 50 m, respectively. In this study, the number of scanning directions and the resolution of the laser pulse were extremely important because TLS measurement was assumed and used as the actual estimates by which the ALS-derived factors of the individual trees could be approximated to the actual value. Therefore, the instrument factors were set as high as possible. Thereafter, the four acquired datasets were integrated into one dataset based on the absolute positions of four sphere balls which were installed on stationary objects before the acquisition of the laser returns (Figure 2).

3. Method

3.1. Extraction of Tree Parameters Using Airborne Laser Scanner Data

3.1.1. Derivation of Crown Height Model

To generate a DTM and DSM, the ALS data were classified into two groups: ground returns and above-ground returns including understory. As the along-track distances were longer than those of across-track, the surface models may potentially have contained false strips in the flying direction, caused by the precipitous difference between neighboring cells when the interpolation is performed to generate the surface model [5]. Therefore, the above-ground returns were filtered with a 1 m × 1 m window to select only the highest points within the window before generating the DTM and CHM. Thereafter, the CHM was computed by subtracting the DTM from the DSM [5].

3.1.2. Crown Delineation

To estimate individual tree parameters, individual trees initially have to be detected and their crown boundaries delineated. The watershed segmentation method was employed because it is a powerful partitioning tool for gray-scale images such as CHM [13]. In image processing, watershed segmentation is an algorithm based on the topology of the image by flooding process which is performed on the gradient image [27]. However, watershed segmentation methods tend to suffer from overestimation and underestimation due to the fluctuant height variation within their topography or hidden treetops of the lower trees under the crowns of the higher trees [5]. In this study, the extended maxima transformation of the image processing method was applied to decrease the incidence of spurious treetops caused by the CHM computed with unfiltered LiDAR returns, whereas Popescu *et al.* [28] and Chen *et al.* used the local-maxima filtering method and marker-controlled watershed segmentation for decreasing detection error [13]. The CHM was segmented for individual crown delineations using the watershed segmentation method after processing the extended maxima transformation. Details of the delineation of individual tree crowns are described in Kwak *et al*. [5].

3.1.3. Estimation of Individual Tree Height and Crown Base Height

To estimate TH and CBH, the process of segmentation was iterated until a one-to-one relationship was achieved between field measurement and detected individual trees. Thereafter, individual TH values were determined to be the highest value of the CHM within the segmented boundaries [29].

Moreover, the *k*-means algorithm was employed for determining and estimating CBH because it was the fastest consistently working method at the individual tree level for the classification of ALS data [16,29]. For determining the CBH, ALS data reflected within individual trees after segmentation were classified into three clusters (ground, understory and crown cluster) using *k*-means clustering [30], since Korean Pine stands included few bi-storied, applicable to the three above-mentioned clusters (Figure 3). The *k*-means statistics applied here is an algorithm used to classify or group attributes or features into *k* number of groups, and uses an iterative algorithm to minimize the sum of the distances (SOD, Equation (1)) from each object (*n*) to its cluster centroid (*i*), over all clusters [31].

$$SOD_{i...k} = \sum_{i}^{k} \left| Centroid_{i...k} - Object[n] \right| \quad (1)$$

where $Centroid_i$ is the mean of the i^{th} cluster of *k* clusters and *object* [*n*] is an observation for a given cluster, *i*. After determining the appropriate clustering level through *k*-means processing, the CBH was determined to be the lowest height within the crown cluster.

Figure 3. Classification of ALS data according to individual trees segmented using the Kwak *et al*. method [5] **(a)**, result of *k*-means clustering for ALS data reflected from individual tree spaces **(b)**, and CGV generated from crown returns **(c)**.

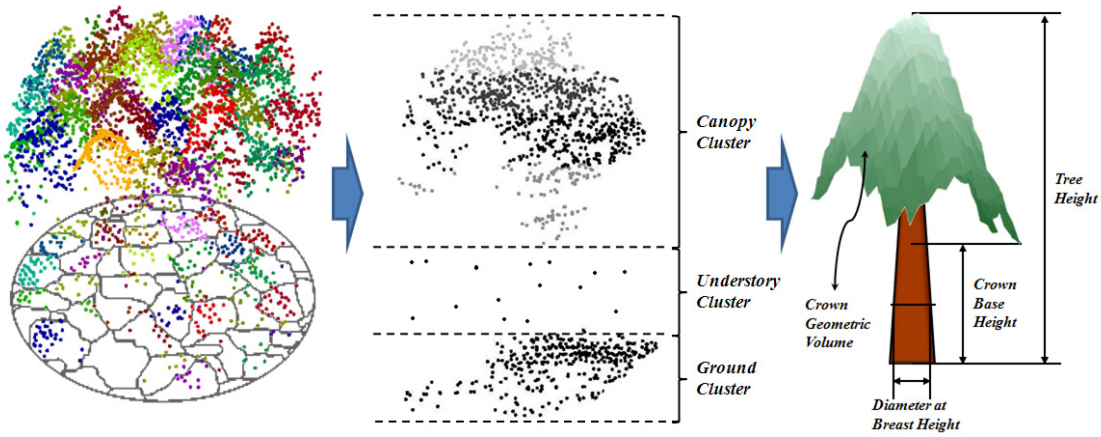

3.1.4. Estimation of Crown Area and Crown Geometric Volume

The crown area (CA) was estimated easily from the boundaries delineated by the extended maxima transformation and watershed segmentation. The crown returns reflected above CBH were transformed to the CHM [32]. The CGV values derived from CHM were calculated using the "Surface Volume Calculation Module" of ArcInfo program [33] (Figure 3(c)).

3.2. Extraction of Tree Parameters Using Terrestrial Laser Scanner Data

3.2.1. Measurement of Tree Height and Crown Base Height

The height of the individual trees was estimated by extracting the highest point data among the entire point data of the individual trees which were integrated with the four directional TLS dataset.

Once the point P(x_i, y_i, z_i) was selected, the coordinates could be calculated in the TLS device coordinate system according to Equation (2) and Figure 4.

$$x_i = d \cdot \cos\alpha \cdot \cos(90 - \beta),\ y_i = d \cdot \cos\alpha \cdot \sin(90 - \beta),\ z_i = d \cdot \sin\alpha \quad (2)$$

where x_i, y_i, z_i are x, y, z coordinates (distances) of the i^{th} point, d the distance from TLS to the i^{th} point in three dimensional space, α the inclination angle to the i^{th} point, and β the azimuth from TLS to the i^{th} point. The distance (d), inclination (α) and azimuth angle (β) from TLS to the i^{th} point were measured automatically in the TLS device system when laser pulses were transmitted and received. However, in the case of detecting CBH by TLS, the k-means clustering method could not be applied due to the identical point density. That's why the TLS point cloud was continuous from the crown to the stem below crown, so that TLS point was not clearly separated. Therefore, we extracted the CBH manually on the screen regarding the lowest point P_j (x_j, y_j, z_j) among the entire crown returns as CBH.

Figure 4. Estimation of tree height (TH) (P_i) and crown base height (CBH) (P_j) using the distance (d) and angles (α and β) between TLS and individual trees.

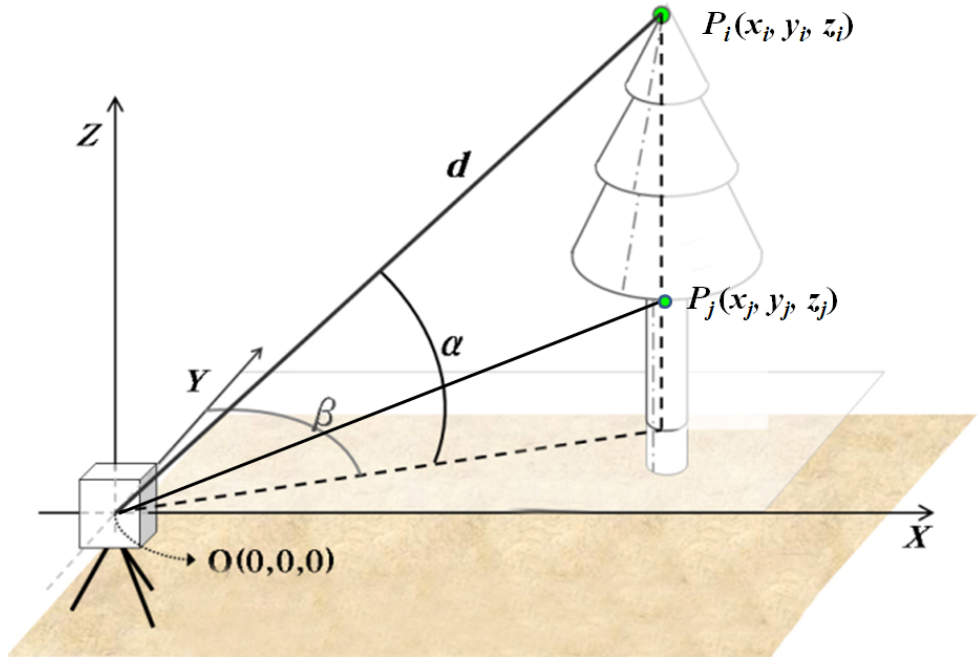

3.2.2. Measurement of Crown Area and Crown Geometric Volume

The measurement of CA and CGV using TLS was complicated because the TLS data were acquired densely through the side observation system, as shown in Figure 4. Therefore, the TLS data of individual trees were reselected as the maximum height by filtering with a moving voxel composed of 1 cm × 1 cm × ∞ (Figure 5). Thereafter, the extracted TLS data were used to generate the CHMs, and then the CGV values of individual trees were computed using the 'surface volume calculation module' of ArcInfo 9.2 software as ALS-computed CGV. The CA values were measured with the projected areas of the CHMs of individual trees that were calculated as shown in Figure 5.

Figure 5. Manually detected individual trees using the TLS data **(a)**, filtered TLS data with moving voxel **(b)**, crown surface returns among the filtered TLS data **(c)**, crown height model (CHM) generated from the crown surface returns **(d)**, and projected shape of CHM **(e)**.

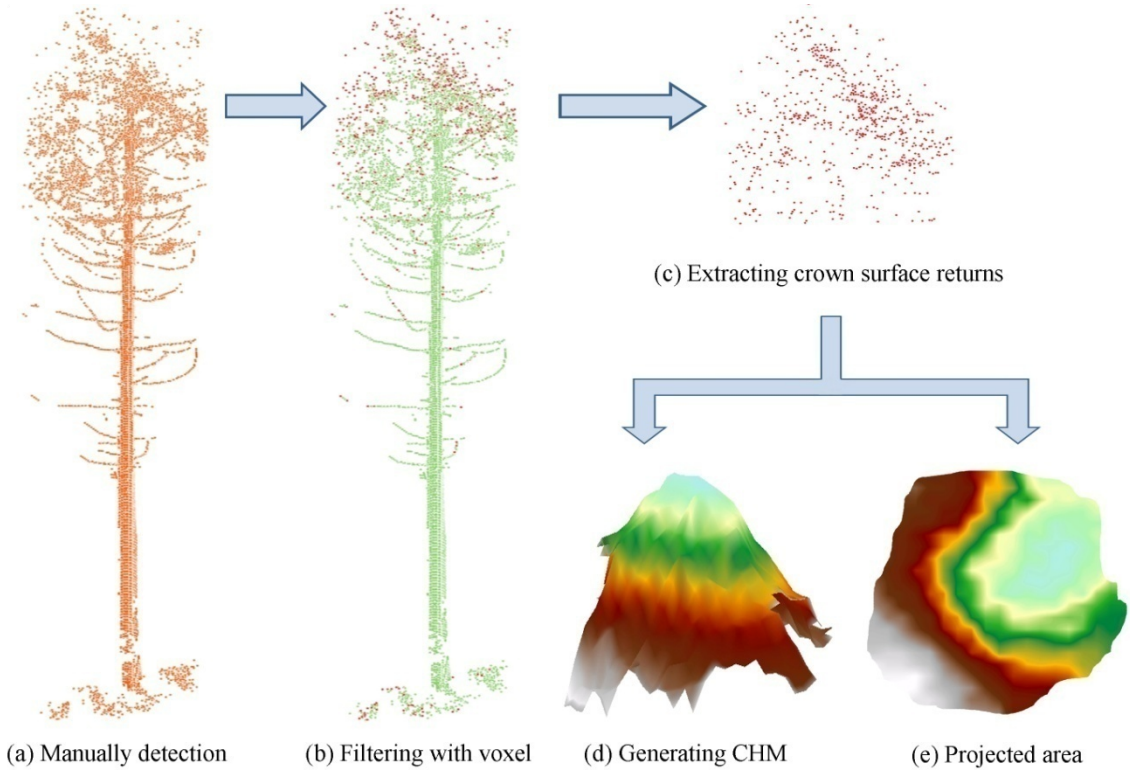

3.3. Regression Analysis and Accuracy Assessment

We assumed that the point density of the TLS data is sufficient to describe an actual shape of the TH, CBH, DBH and crown of individual trees [20-22,24]. Therefore, the TLS-derived TH, CBH, CA and CGV were used for ground reference data to perform simple regression analysis with ALS estimates. Prior to regression analysis between TLS and ALS estimates, one-to-one individual tree relationship was established by overlaying each individual tree tops derived from each LiDAR systems through matching the GPS coordinate of TLS with ALS coordinate systems. The dislocated individual trees from ALS were compulsively matched with the closest individual trees derived from TLS.

$$Parameter_{TLS} = \alpha \cdot Parameter_{ALS} + \beta \quad (3)$$

where, $Parameter_{TLS}$ and $Parameter_{ALS}$ are TLS- and ALS-extracted TH, CBH, CA and CGV, respectively.

To assess the accuracy of the developed regression function, 15 Korean Pines were subjected to TLS measurements. The parameters estimated by the regressed functions were statistically compared with the TLS measurement data using the coefficient of determination (R^2) and root mean square error (RMSE). Finally, the developed regression functions were used to correct the ALS-estimated parameters. Thereafter, the error rate was used to determine the extent to which the ALS-caused errors would be improved by the application of the regression models (Equation (4)).

$$Error = \left| \frac{Parameter_{OBS} - Parameter_{PRE}}{Parameter_{OBS}} \right| \quad (4)$$

where, $Parameter_{OBS}$ and $Parameter_{PRE}$ are TH, CBH, CA and CGV observed and predicted by TLS and ALS respectively.

4. Results and Discussions

4.1. Tree Height

In the regression analysis results with ALS- and TLS-derived TH, R^2 and RMSE were 0.9361 and 0.6016, respectively, and the coefficients α_{TH} and β_{TH} were estimated to be 0.8729 and 2.2995, respectively (Table. 2).

Table 2. Results of regression analysis on ALS- and TLS-derived TH, CBH, CA and CGV.

Parameters	Coefficient	Estimate	Standard Error	*T* statistics	*P* value	R^2	RMSE
TH	α_{TH}	0.8729	0.0632	13.9000	<0.0001	0.9361	0.6016 (m)
	β_{TH}	2.2995	1.0633	2.1600	0.0498		
CBH	α_{CBH}	1.1115	0.1795	6.1900	<0.0001	0.7468	1.8742 (m)
	β_{CBH}	−0.7137	1.6226	−0.4400	0.6673		
CA	α_{CA}	0.9471	0.1752	5.4100	<0.0001	0.6923	6.8435 (m^2)
	β_{CA}	6.4687	4.8759	1.3300	0.2074		
CGV	α_{CGV}	72.6232	17.2458	4.2111	0.0010	0.5770	31.7109 (m^3)
	β_{CGV}	−196.7759	83.5614	−2.3549	0.0349		

The ALS- and TLS-derived mean TH values were estimated to be 16.6 m and 16.8 m, respectively. The underestimation of ALS was attributed to the possibly low probability of the laser pulses emitted from ALS being reflected on real tree tops [5,17]. In general, it is more difficult for laser pulses to be reflected on precise tree tops due to the conical crown shape of coniferous trees [34]. However, we assumed that TLS-measured THs could be used for reference data, because few TLS-derived measurements were lower than those of ALS (Figure 6(a)) and TLS could measure the object with 2 mm [26].

The R^2 and RMSE values used to verify the results were assessed to be 0.9348 and 0.0184 m, respectively (Figure 6(b)). The mean of the observed and predicted TH was estimated at 16.1 m. This result differed from that of the TH used in the regression analysis because the prediction estimated through ALS-derived TH could approach the TH-derived TLS. From this tendency, the error rate change was calculated to be −0.0089 by subtracting the uncorrected (0.0270) from the corrected (0.0181) error rate (Figure 6(c)).

Figure 6. Reduction of TH-estimate errors through the regression model.

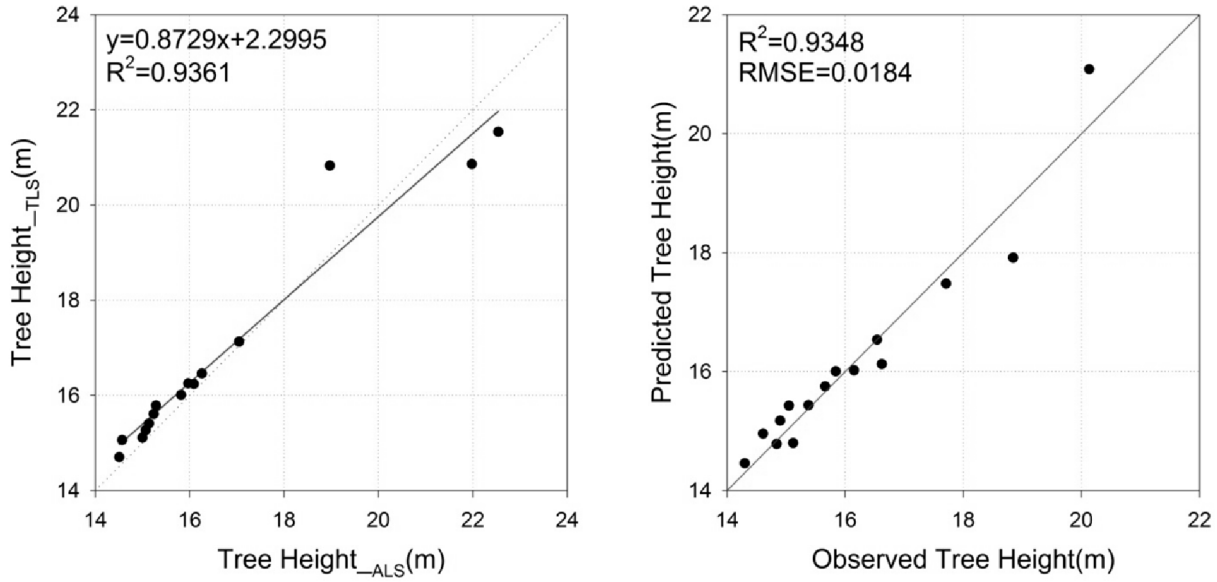

(a) Regression analysis **(b)** Verification

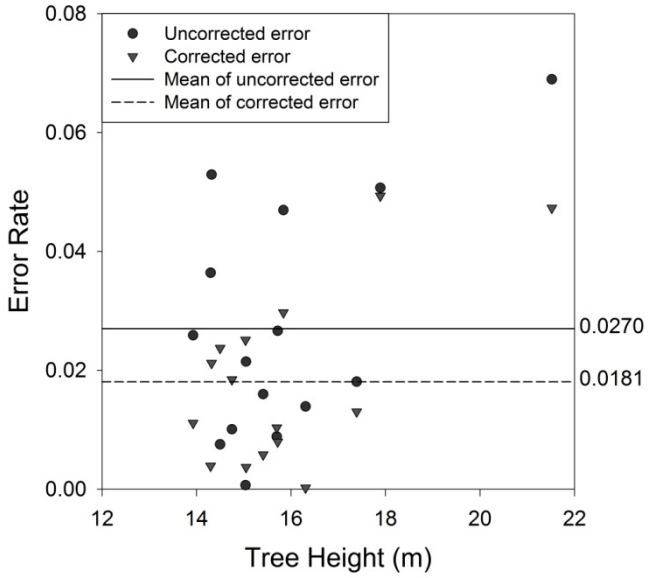

(c) Decrement of errors

4.2. Crown Base Height

The *k*-means clustering was used to classify the LiDAR returns into three clusters: ground, understory and crown cluster. Thereafter, the ALS-extracted CBH could be estimated at the lowest height of a crown cluster. On the other hand, the TLS measurement was performed manually on the screen like the TLS-derived TH. Linear regression analysis was conducted to determine the relationship between the ALS- and TLS-derived CBH values. The R^2 and RMSE values were calculated to assess the accuracy of the regression analysis (Table. 1).

In this study, the ALS- and TLS-derived mean CBH values of individual trees were analyzed to be 8.8 m and 8.6 m, respectively. However, the ALS-derived CBH generally tended to be higher than the actual CBH. That was attributed to the inability to detect the real CBH under the overlapping crown

edges between neighboring trees [30,35,36]. Likewise, most of the ALS-estimated CBH values were higher than those of TLS in this study.

The accuracy of the regression function was evaluated by R^2 and RMSE values of 0.8273 and 0.4929 m, respectively (Figure 7(b)). However, the error rate did not show any decrement by the regressed function (Figure 7(c)) due to the insufficiency of unbiased data for the verification. Furthermore, the measurement error in the field was also strongly attributable to the overlapping trees.

Figure 7. Reduction of CBH-estimate errors through the regression model.

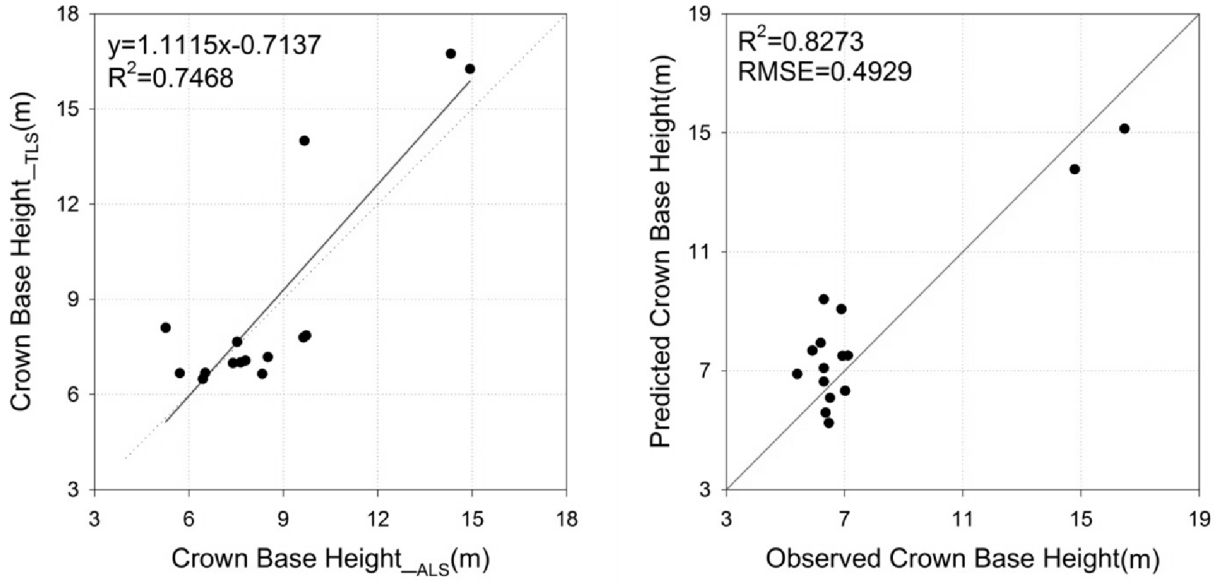

(a) Regression analysis **(b)** Verification

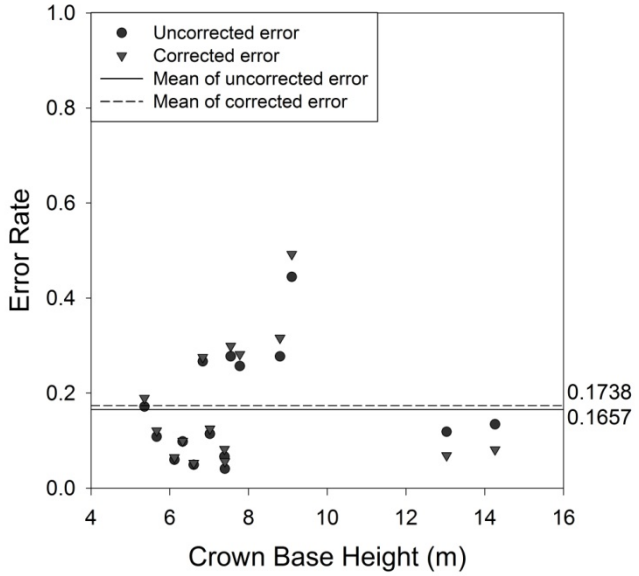

(c) Decrement of errors

4.3. Crown Area

The R^2 and RMSE values obtained through regression analysis were 0.6923 and 6.8435 m^2, respectively, and the coefficients α_{CBH} and β_{CBH} were estimated to be 0.9471 and 6.4687, respectively.

The ALS- and TLS-derived mean CA values were 25.9 m^2 and 31.0 m^2, respectively. The TLS-derived CA values were mostly larger than those of ALS because TLS could acquire extremely dense laser returns from four sides of individual trees. Therefore, TLS-emitted laser pulses can describe the entire crown shape, including an actual CBH, which is the real boundary of the individual tree crown. On the other hand, ALS records the reflected pulses vertically with a low point density from the crowns of individual trees to the ground. Therefore, ALS pulses are reflected on the upper crown part, but rarely around CBH (Figure 8(c)).

Figure 8. Reduction of CA-estimate errors through the regression model.

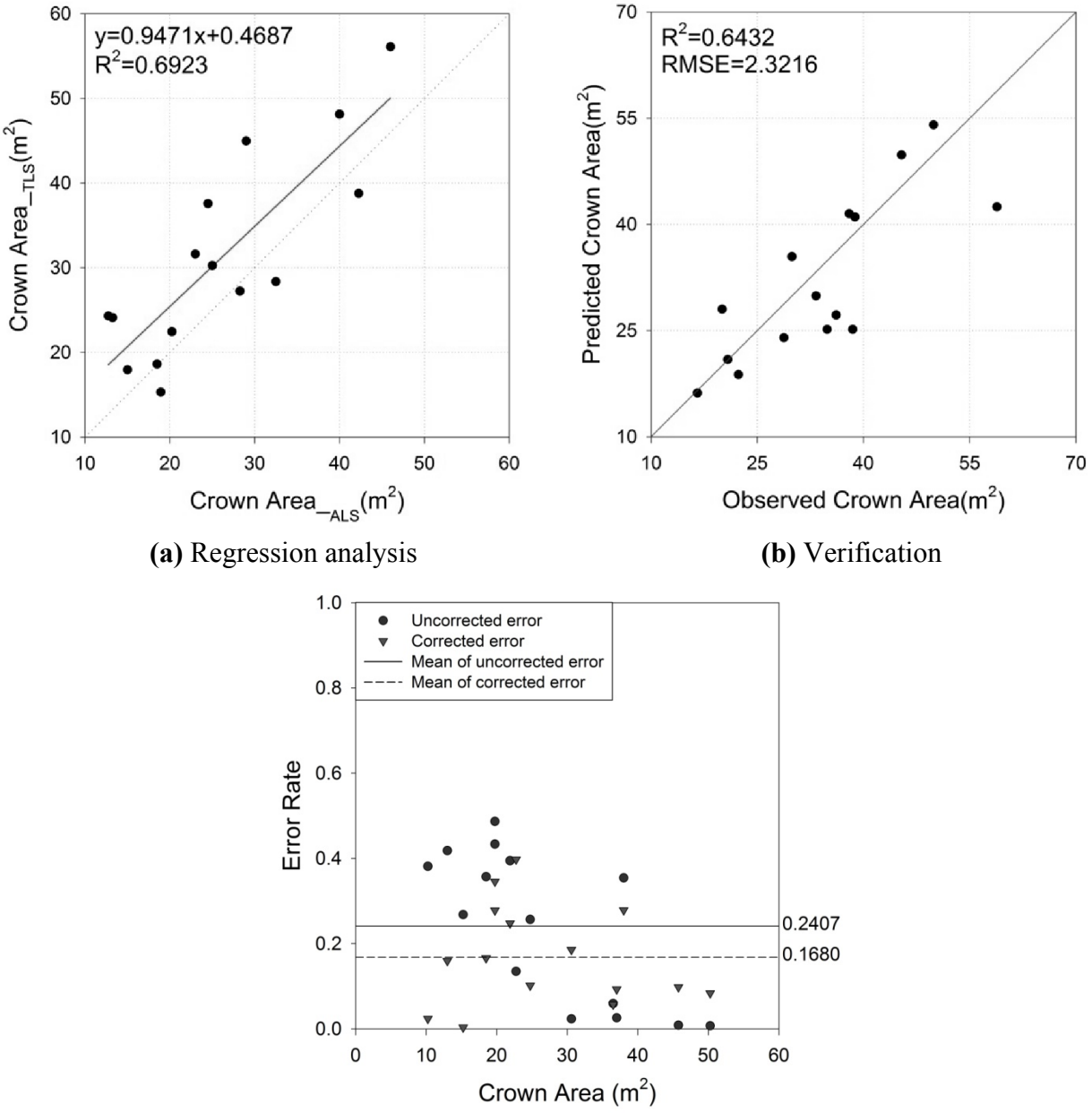

(a) Regression analysis **(b)** Verification

(c) Decrement of errors

The R^2 and RMSE values for the verification were 0.6432 and 2.3216 m^2, respectively, and the error rate was decreased from 0.2407 before applying the regression model to 0.1680 afterwards, *i.e.*, a difference of −0.0727 between the uncorrected and corrected estimations.

4.4. Crown Geometric Volume

The ALS-derived CGV values were estimated from the CHMs of the individual trees segmented. The TLS-derived CGV values were computed from the CHMs generated with only crown surface returns filtered with a moving voxel. The ALS- and TLS-derived CGV values were used for the regression analysis. In the results, R^2 and RMSE were evaluated to be relatively low at 0.5770 and 31.7109 m^3, respectively, when compared with TH, CBH and CA (Table. 1). The mean ALS- and TLS-derived CGV values were estimated to be 139.0 m^3 and 153.4 m^3, respectively. The difference of the mean CGV values was also attributed to the uncertainty due to the overlapping effect and the underestimation of the ALS-derived TH.

Figure 9. Reduction of CGV-estimate errors through the regression model.

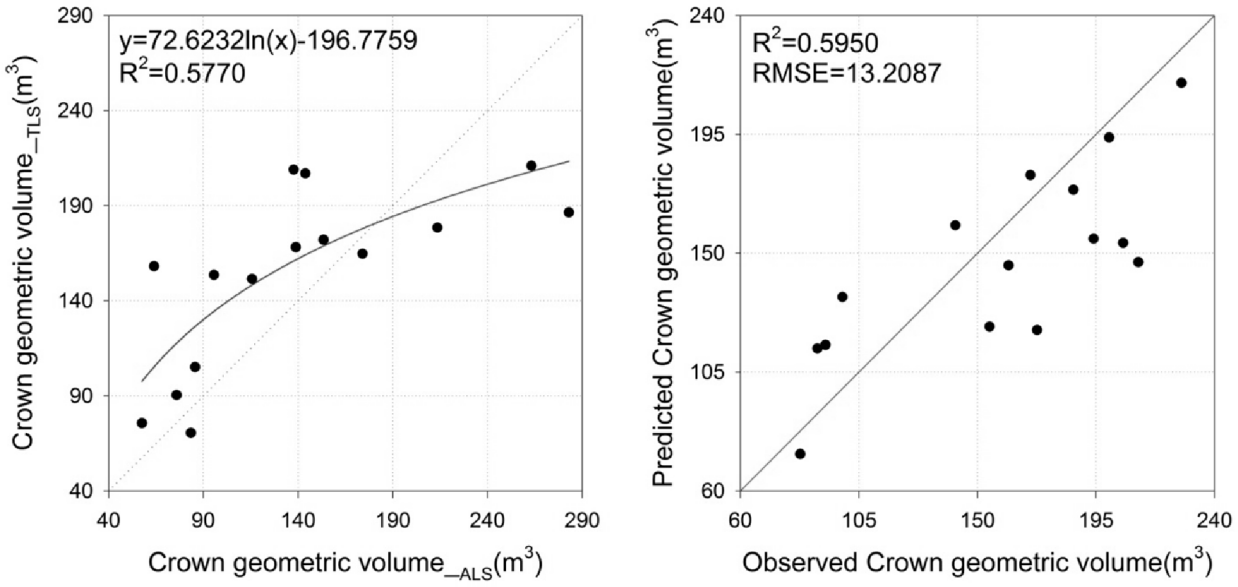

(a) Regression analysis **(b)** Verification

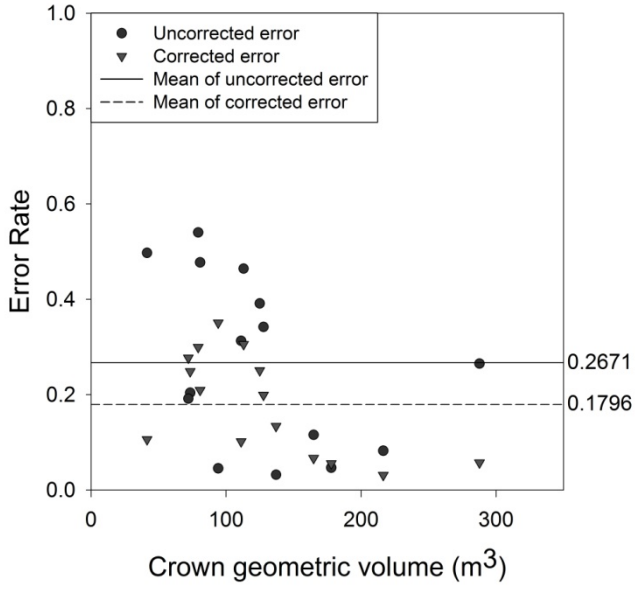

(c) Decrement of errors

In particular, the regression model for CGV showed a natural logarithm form (Figure 9(a)), which revealed the limitation of ALS estimation for CA and CGV. Specifically, in the current status of forest stand surveyed for this study, the increment of the actual CA accompanied greater overlapping of CA between neighboring trees. However, the ALS-estimated CA could not increase continuously because the ALS-derived CA may have been seriously underestimated due to the over-segmentation caused by the extreme crown overlapping.

The R^2 and RMSE values and the uncorrected and corrected error rates for the verification of the regression model were 0.5950, 13.2087 m^3, 0.2671 and 0.1796, respectively (Figure 9(b)). Their variation after the application of the regression model also demonstrated the reduced effectiveness in the parameters such as TH, CBH and CA.

4.5. Overall Analysis

The study results were analyzed in the comparison of various statistics with improving the accuracies in TH, CA and CGV measurements. When performing this study, some limitations arose in estimating the parameters with ALS and TLS. The first limitation was the difficulty in estimating the actual ALS-derived CBH due to the blockage of the lowest branches when higher branches were longer than that within an individual tree, as shown in Figure 10. Popescu (2008) and Chasmer (2006) have already noted that laser pulses delineating crowns from above and lower branches have a low probability of reflecting on actual crown boundaries due to obstruction by higher branches [37,38]. These effects can lead to the overestimation of CBH and the underestimation of CA and CGV (Figure 10).

Figure 10. Misinterpretation in measuring CBH due to obstruction by higher branches when ALS data are used.

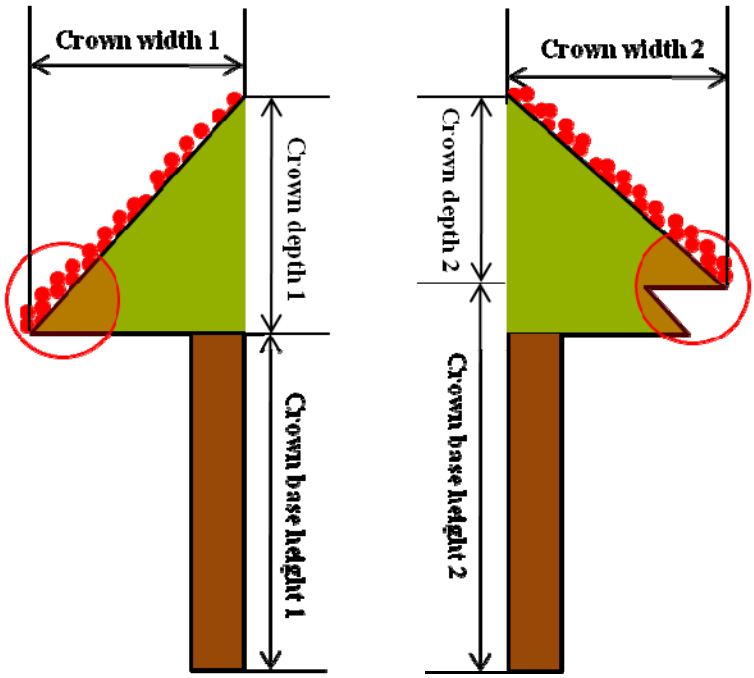

The second limitation was the overlapping effect between the objective tree and its neighbors, which may have led to the underestimation of the crown diameter and area by partitioning individual trees along the valley between the crowns. In particular, the ALS-derived CBH might have been underestimated due to the overlapping between neighboring trees in a dense forest stand. Moreover, such overlapping causes a major problem in underestimating CA and CGV, leading to ambiguity in their accuracies. As shown in Figure 11, when occupied areas are supposed to be equal, a low tree density could lead to small overlapping frequency and area. However, the overlapping errors accumulate with increasing number of trees. These increasing errors can cause other errors when estimating forest growth parameters, such as TH, CBH, CA and CGV. The relatively overlapped area of a crown edge increases according to the tree density due to the reduction in crown width with decreasing growing space. ALS-derived forest growth factors are easily underestimated when compared to field measurements. Therefore, overlapping-removal models according to the tree density must be considered in future studies.

Figure 11. Relationship between overlapping effect level and low **(a)**, medium **(b)**, and high **(c)** tree density.

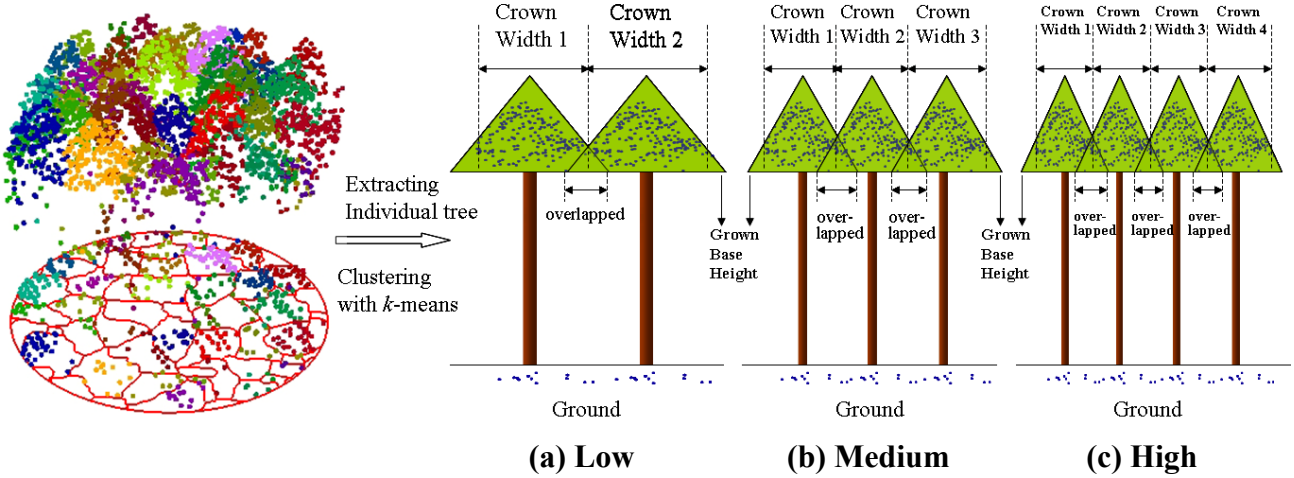

In spite of same dataset, the error rate of CBH showed the increment whereas those of other parameters were improved. The reason can be explained with the independent estimation of TLS-derived CBHs. CBHs of individual trees are distributed between about 5~7 m in Figure 7 while their TLS-derived TH, CA and CGV have various estimates in Figures 6, 8 and 9. This is attributed to the fact that TLS-derived THs, CAs and CGVs can be estimated variously even if the trees have similar CBHs. Namely, TLS-derived CBHs are estimated independently from TLS-derived CHMs. Moreover, TLS-derived TH, CA and CGV were not estimated through the regression model which has CBH of independent variable. Therefore, CBHs do not influence to the estimation of TLS-extracted THs, CAs and CGVs, and the error rate of their parameters cannot follow the tendency of CBHs in this study. In particular, the error rates of CBHs were improved little when compared with those of other parameters. That is why the measurement of CBHs by ALS is more affected by the overlapping than that of THs, CAs and CGVs. Therefore, similar TLS-derived observations have various predictions as shown in Figure 7.

6. Conclusions

In this study, we estimated several tree parameters and developed regression models for improving the accuracy of estimating parameters using ALS and TLS. In the results, the estimated ALS-derived TH value was lower than that of TLS because of a few cases of reflection on tree tops in the case of ALS. The estimated ALS-derived CBH value was higher than that of TLS due to the almost complete interception in the upper part of the trees, except for a few trees. The ALS-derived CA and CGV values were underestimated when compared with those of TLS because of the overlapping effect induced by neighboring trees in the aircraft-acquired data. After the extraction of the tree parameters, we developed regression functions by assuming the TLS-derived parameters to be the ground reference data. The equations were relatively meaningful as assessed by various statistics. Therefore, with the approximations being validated as close to the real values, each coefficient extracted from the regression models was used to correct the ALS-estimated values. We evaluated the model accuracy to determine the effectiveness of the improving error rate. In the accuracy assessment results, all the tree parameters except CBH showed an improvement in error rate through the regression model. The error rate of CBH was not decreased by the regressed function due to insufficient unbiased data for verification. Most importantly, however, most of the estimated tree parameters were significantly improved.

The ALS- and TLS-derived estimations of the tree parameters suffered from the following two limitations. Firstly, the overlapping between an objective tree and its neighbors may have influenced the estimation of tree parameters using ALS. Moreover, laser pulses have a low probability of reflecting on actual crown boundaries due to obstruction by higher branches. Secondly, the point density of the LiDAR data influences the accuracy of the estimated forest growth factors when the points are distributed systematically, or the point density is insufficient to describe individual tree crown shapes. If such error-causing problems can be corrected, more accurate results will be obtained in the extraction of forest growth factors using ALS and TLS data.

Acknowledgements

This study was carried out with the support of ‘‘Forest Science and Technology Projects (Project No. S120911L010130)’’ provided by Korea Forest Service.

References

1. Koch, B.; Heyder, U.; Welnacker, H. Detection of individual tree crowns in airborne lidar data. *Photogramm. Eng. Remote Sensing* **2006**, *4*, 357-363.
2. Avery, T.E.; Burkhart, H.E. *Forest Measurements*, 4th ed.; McGraw–Hill: Boston, MA, USA, 1994.
3. Shivers, B.D.; Borders, B.E. *Sampling Techniques for Forest Resource Inventory*, 1st ed.; Wiley: New York, NY, USA, 1996.
4. Lefsky, M.A.; Cohen, W.B.; Parker, G.G.; Harding, D.J. LiDAR remote sensing for ecosystem studies. *Bioscience* **2002**, *52*, 19-30.

5. Kwak, D.A.; Lee, W.K.; Lee, J.H.; Biging, G.S.; Gong, P. Detection of individual trees and estimation of tree height using LiDAR data. *J. Forest Res*. **2007**, *12*, 425-434.
6. Lefsky, M.A.; Cohen, W.B. Selection of remotely sensed data. In *Remote Sensing of Forest Environments, Concepts and Case Studies*, 1st ed.; Wulder, M.A., Franklin, S.E., Eds.; Kluwer Academic Publishers: Norwell, MA, USA, 2003; pp.13-46.
7. Dubayah, R.O.; Drake, J.B. Lidar remote sensing for forestry. *J. Forest.* **2000**, *98*, 44-46.
8. Aldred, A.; Bonnor, M. *Application of Airborne Lasers to Forest Surveys*; Information Report PI-X-51; Canadian Forestry Service, Petawawa National Forestry Centre: Chalk River, ON, Canada, 1985; p. 62.
9. MacLean, G.A.; Martin, G.L. Merchantable timber volume estimation using cross-sectional photogrammetric and densitometric methods. *Can. J. Forest Res.* **1984**, *14*, 803-810.
10. Nelson, R. Determining forest canopy characteristics using airborne laser data. *Remote Sens. Environ.* **1984**, *15*, 201-212.
11. Næsset, E. Determination of mean tree height of forest stands using airborne laser scanner data. *ISPRS J. Photogramm.* **1997**, *52*, 49-56.
12. Magnussen, S.; Boudewyn, P. Derivations of stand height from airborne laser scanner data with canopy-based quantile estimators. *Can. J. Forest Res.***1998**, *28*, 1016-1031.
13. Chen, Q.; Baldocchi, D.; Gong, P.; Kelly, M. Delineating individual trees in a Savanna Woodland using small footprint LiDAR data. *Photogramm. Eng. Remote Sensing* **2006**, *72*, 923-932.
14. Næsset, E. Estimating timber volume of forest stands using airborne laser scanner data. *Remote Sens. Environ.* **1997**, *61*, 246-253.
15. Lim, K.; Treitz, P.; Baldwin, K.; Morrison, I.; Green, J. LiDAR remote sensing of biophysical properties of tolerant northern hardwood forests. *Can. J. Remote Sens.* **2003**, *29*, 658-678.
16. Kwak, D.A.; Lee, W.K.; Cho, H.K.; Lee, S.H.; Son, Y.; Kafatos, M.; Kim, S.R. Estimating stem volume and biomass of *Pinus koraiensis* using LiDAR data. *J. Plant Res.* **2010**, *123*, 421-432.
17. Zimble, D.A.; Evans, D.L.; Carlson, G.C.; Parker, R.C.; Grado, S.C.; Gerardd, P.D. Characterizing vertical forest structure using small-footprint airborne LiDAR. *Remote Sens. Environ*. **2003**, *87*, 171-182.
18. Parker, G.G.; Harding, D.J.; Berger, M.L. A portable LIDAR system for rapid determination of forest canopy structure. *J. Appl. Ecol.* **2004**, *41*, 755-767.
19. Tickle, P.K; Lee, A.; Lucas, R.M.; Austin, J.; Witte, C. Quantifying Australian forest floristics and structure using small footprint LiDAR and large scale aerial photography. *Forest Ecol. Manage.* **2006**, *223*, 379-394.
20. Hopkinson, C.; Chasmer, L.; Young-Pow, C.; Treitz, P. Assessing plot level metrics with a ground-based scanning LiDAR. *Can. J. Remote Sens*. **2004**, *34*, 573-583.
21. Thies, M.; Spoecker, H. Evaluation and future prospects of terrestrial laser scanning for standardized forest inventories. *ISPRS J. Photogramm.* **2004**, *36*, 192-197.
22. Simonse, M.; Aschoff, T.; Spiecker, H.; Thies, M. Automatic Determination of Forest Inventory Parameters Using Terrestrial Laserscanning. In *Proceedings of the ScandLaser Scientific Workshop on Airborne Laser Scanning of Forests*, Umeå, Sweden, 3–4 September 2003; pp. 251-257.

23. Chen, Q.; Gong, P.; Baldocchi, D.; Tian, Y.Q. Estimating basal area and stem volume for individual trees from LiDAR data. *Photogramm. Eng. Remote Sensing* **2007**, *73*, 1355-1365.
24. Watt, P.J.; Donoghue, D.N.M.; Dunford, R.W. Forest Parameter Extraction Using Terrestrial Laser Scanning. In *Proceedings of the ScandLaser Scientific Workshop on Airborne Laser Scanning of Forests*, Umeå, Sweden, 3–4 September 2003; pp. 237- 244.
25. Henning, J.G.; Radtke, P.J. Detailed stem measurements of standing trees from ground-based scanning lidar. *Forest Sci.* **2006**, *52*, 67-80.
26. Trimble Home Page. GS200 3D Scanner. Available online: www.trimble.com/gs200.shtml (accessed on 22 September 2010).
27. Soille, P. *Morphological Image Analysis: Principles and Applications*, 2nd ed.; Springer-Verlag: Berlin, Germany, 2003; p. 391.
28. Popescu, S.C.; Wynne, R.H.; Scrivani, J.A. Fusion of small footprint LiDAR and multispectral data to estimate plot-level volume and biomass in deciduous and pine forests in Virginia, USA. *Forest Sci*. **2004**, *50*, 551-565.
29. Hyyppä, J.; Kelle, O.; Lehikoinen, M.; Inkinen, M. A segmentation based method to retrieve stem volume estimates from 3-D tree height models produced by laser scanners. *IEEE Trans. Geosci. Remote* **2001**, *39*, 969-975.
30. Riano, D.; Chuvieco, E.; Condis, S.; Gonzalez-Matesanz, J.; Ustin, S. L. Generation of crown bulk density for Pinus sylvestris from LIDAR. *Remote Sens. Environ*. **2004**, *92*, 345-352.
31. MATLAB. *Help Documents in MatLab 2006*; Mathwork: Natick, MA, USA, 2006.
32. Chen, Q.; Gong, P.; Baldocchi, D.D.; Xie, G. Filtering airborne laser scanning data with morphological methods. *Photogramm. Eng. Remote Sensing* **2007**, *73*, 171-181.
33. ArcGIS. *Help Documents in ArcGIS 8.1*; Environmental Systems Research Institute (ESRI): Redlands, CA, USA, 2001.
34. Coder, K.D. *Crown Shape Factor & Volumes*; Tree Biomechanics 672 Series; University of Georgia: Athens, GA, USA, 2000; pp. 1-5.
35. Kwak, D.A.; Lee, W.K.; Cho, H.K.; Lee, S.H. Estimation of Tree Volume Using LiDAR Remote Sensing. In *Proceeding of the A3 Foresight Program (Ecological Processes for Carbon Cycling: Temporal and Spatial Variations)*, Jinju, Korea, 21–23 April 2009; pp. 49-52.
36. Holmgren, J.; Persson, Å. Identifying species of individual trees using airborne laser scanner. *Remote Sens. Environ.* **2004**, *90*, 415-423.
37. Popescu, S.C.; Zhao, K. A voxel-based lidar method for estimating crown base height for deciduous and pine trees. *Remote Sens. Environ*. **2008**, *112*, 767-781.
38. Chasmer, L.; Hopkinson, C.; Treitz, P. Investigating laser pulse penetration through a conifer canopy by integrating airborne and terrestrial lidar. *Can. J. Remte Sens.* **2006**, *32*, 116-125.